



The effects of Hurricanes Katrina and Rita on seabed polycyclic aromatic hydrocarbon dynamics in the Gulf of Mexico

Siddhartha Mitra^{a,*}, Joseph J. Lalicata^{a,1}, Mead A. Allison^{b,2}, Timothy M. Dellapenna^c

^a Department of Geological Sciences and Environmental Studies, Binghamton University, Binghamton, NY 13902-6000, United States

^b Department of Earth and Environmental Sciences, Tulane University, New Orleans, LA 70118, United States

^c Department of Oceanography, Texas A&M University at Galveston, P.O. Box 1675, Galveston, TX 77553, United States

ARTICLE INFO

Keywords:

Hurricanes
Sediment resuspension
PAH
Gulf of Mexico
Seabed dynamics

ABSTRACT

To assess the extent to which Hurricanes Katrina and Rita affected polycyclic aromatic hydrocarbons (PAH) in the Gulf of Mexico (GOM), sediment cores were analyzed in late 2005 from: a shallow shelf, a deeper shelf, and a marsh station. Sediment geochronology, fabric, and geochemistry show that the 2005 storms deposited ~10 cm of sediment to the surface of a core at 5-12A. Bulk carbon geochemistry and PAH isomers in this top layer suggest that the source of sediment to the top portion of core 5-12A was from a relatively more marine area. Particulate PAHs in the marsh core (04 M) appeared unaffected by the storms while sediments in the core from Station 5-1B (deeper shelf) were affected minimally (some possible storm-derived deposition). Substantial amounts of PAH-laden particles may have been displaced from the seabed in shallow areas of the water column in the GOM by these 2005 storms.

© 2009 Elsevier Ltd. All rights reserved.

1. Introduction

Hurricanes have the ability to substantially impact coastal sediment dynamics. The energy of a strong storm can cause large waves, as well as strong currents, both of which have the ability to disperse and resuspend large volumes of sediments (Parsons, 1998; Ogston et al., 2000; Dail et al., 2007). In 2005, two such intense storms, Hurricanes Katrina and Rita entered the Gulf of Mexico (GOM). Hurricane Katrina and Rita both eventually reached Category 5 status on the Saffir-Simpson scale. Hurricane Katrina which struck land on August 29, 2006 had a storm surge of 1.5–3 m in southern Louisiana (Van Biersel et al., 2007) while Hurricane Rita which struck land on September 24, 2006, had a storm surge that averaged 1 to 5 m throughout Louisiana (Goni et al., 2007). The powerful nature of Hurricanes Katrina and Rita resulted in extensive resuspension followed by erosion and deposition of sediment throughout near-shore and offshore portions of the seabed in the GOM (Walsh et al., 2006).

The GOM is an important habitat and contains an extensive series of harbors as well as infrastructure supporting the offshore petroleum industry, all of which are frequently subjected to storms

(Bianchi et al., 1999). While studies have addressed how the 2005 hurricanes affected the nature and extent of seabed sediment dynamics (Walsh et al., 2006) and bulk organic carbon (OC) dynamics (Goni et al., 2007), there have not been any studies addressing the extent to which the 2005 storm season-driven resuspension affected trace contaminant dynamics in the seabed of the GOM. Resuspension of bed sediments can be a significant source of sediment-bound contaminants to the overlying water column (Achman et al., 1996; Niedoroda et al., 1996; Mitra et al., 1999). If the 2005 storms had such a severe effect on sediment dynamics throughout coastal regions of the GOM, then they also could have substantially affected sedimentary contaminant dynamics.

Trace organic contaminants such as polycyclic aromatic hydrocarbons (PAHs) have been quantified in sediments of the GOM prior to the hurricanes (Kennicutt II et al., 1988; Macdonald et al., 1996; Maruya et al., 1997; Mitra and Bianchi, 2003; Turner et al., 2003; Overton et al., 2004). We analyzed PAHs in conjunction with biomarkers of sedimentary organic matter provenance in three sediment cores, collected soon after the 2005 hurricanes. Our objective was to address how the 2005 hurricanes may have affected sedimentary contaminant dynamics in the GOM.

2. Methods

2.1. Sampling

Sediment samples analyzed in this study were collected as part of a larger sampling effort dedicated to understanding seabed

* Corresponding author. Address: Department of Geological Sciences, East Carolina University, Greenville, NC 27858, United States. Tel.: +1 252 328 6611; fax: +1 252 328 4391.

E-mail address: mitras@ecu.edu (S. Mitra).

¹ Present address: Department of Earth Science, University of California, Webb Hall, BLDG 526, Santa Barbara, CA 93106-9630, United States.

² Present address: Institute for Geophysics, University of Texas at Austin, Austin, TX 78758-4445, United States.

dynamics in the near-shore and offshore areas of the GOM immediately following Hurricanes Katrina and Rita. Sediment samples were collected with box corers and Kastan-type gravity corers onboard the R/V *Cape Hatteras* and R/V *Longhorn* on September 26, 2005 (Goni et al., 2007). To address our experimental objective noted above, we obtained three cores from areas in the GOM that we suspect were affected by the 2005 hurricanes. Cores were collected from the inner and mid-shelf of the GOM, and from a coastal marsh in the Mississippi Delta (Fig. 1, Table S1). Cores from Station 5-12A (inner shelf; water depth = 32 m) and 5-1B (mid-shelf; water depth = 80 m) were collected using a box corer (30 cm × 30 cm × 50 cm) within which a 15.24 cm diameter PVC core tube was inserted. A core from a marsh in the eastern portion of the bird's foot delta (Station 04 M) was collected by pushing a PVC core tube directly into subaerial marsh surface sediment. Core 5-12A was sectioned into 1 cm intervals up to 12 cm, while the lower portion of the core was sectioned into 2 cm intervals. Core 5-1B was extruded in 1 cm intervals but only every other interval was subjected to geochemical analyses. The top 12 cm of core 04 M was sectioned into 1 cm intervals, while the lower portion of the core was sectioned into either 2 or 3 cm intervals. Sediment samples were homogenized and stored frozen in pre-ashed (450 °C for 4 h) glass vials until analysis and quantification of organics in the laboratory.

2.2. Radionuclide profiles and X-radiography

Activities of the particle-reactive radiotracer ^7Be were measured using a Canberra[™] planar, intrinsic germanium (LeGe) detector, coupled with a multichannel analyzer. Samples were freeze-dried, ground and sealed into 70 mm diameter Petri dishes, and counted for ~24 h. Wet and dry weights were utilized to determine porosity assuming a particle density of 2.65 g/cm³. Activities were measured using net counts under the gamma peak at 477 keV. Samples were recounted after at least 21 days to allow ^{210}Pb activities to grow to secular equilibrium. Activities of ^{137}Cs were determined as well in this second count using the 661.6 keV photopeak. Total ^{210}Pb activity was determined from the 46 keV photopeak and supported ^{210}Pb activities were determined by using averaged activities of the ^{226}Ra daughters ^{214}Pb (295 and 352 keV) and ^{214}Bi (609 keV). Net count rates of all radiotracers were converted to activities using detector efficiencies obtained by sediment standards (IAEA-300 Baltic Sea); detector backgrounds at each energy of interest were determined using Petri dish blanks (Cutshall et al., 1983), with sediment standards at the specific gamma-ray energies. Subcores were X-rayed with a Kramex PN-20 portable unit operating at 15 keV/70 ma. Standard dark room procedures were used to develop X-radiographs, after

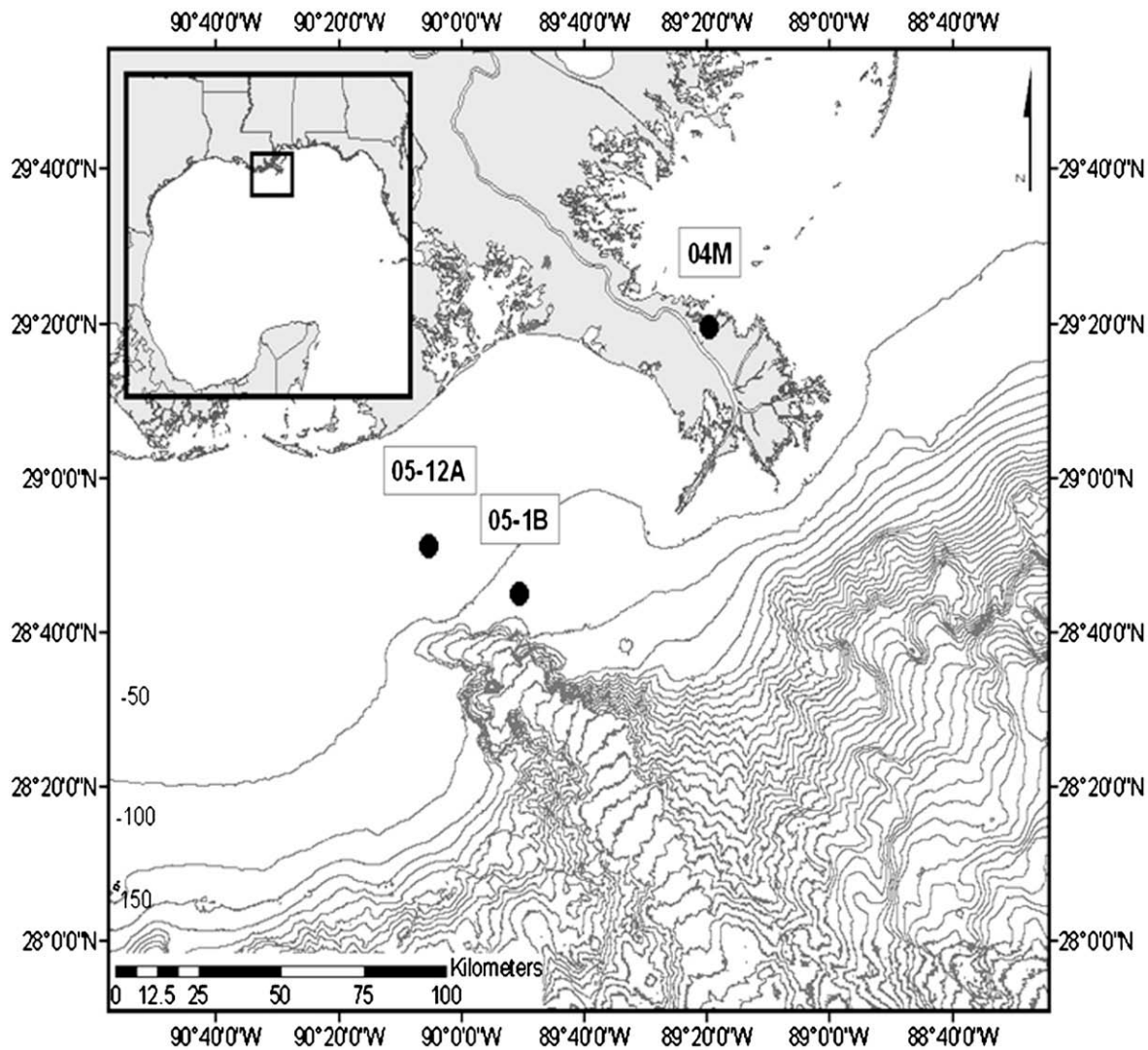


Fig. 1. Site map and sampling locations for the Gulf of Mexico.

which the developed X-radiographs were scanned using a transparency scanner for conversion to digital formats.

2.3. Bulk carbon, nitrogen, and stable isotopes

Analyses for OC and nitrogen (N) abundance and carbon isotopic values were performed at the University of California-Davis Stable Isotope Laboratory measured on a continuous flow Isotope Ratio Mass Spectrometer. Prior to analysis, inorganic carbon was removed from each pre-weighed sediment sample by placing the sample in a glass vial within a dessicator, along with a 40 mL beaker of concentrated HCL (Harris et al., 2001). Samples were removed after there was no further change in weight, ~5 days. Subsamples were then placed in pre-ashed Ag capsules, crimped, and sent for quantification of carbon and nitrogen abundance and their isotopic signature. Ratios of $^{13}\text{C}/^{12}\text{C}$ are expressed in conventional per mille units (‰) relative to the Pee Dee Belemnite (PDB) standard.

2.4. Polycyclic aromatic hydrocarbons

Between 3 and 5 grams of dried and ground sediment were placed in 35 mL Pyrex centrifuge tubes and spiked with a surrogate standard solution of deuterated PAHs, including d_{10} -anthracene, d_{12} -benzo(a)anthracene, and d_{12} -benzo(a)pyrene. Samples were then extracted three times sequentially using a mixture of methylene chloride:methanol $\text{CH}_2\text{Cl}_2/\text{CH}_3\text{OH}$ in a microwave assisted solvent extractor (MASE) (2:1, v:v) (Arzayus et al., 2001). Temperature in the MASE was ramped from room temperature (~23 °C) to 115 °C in 8 min and held for 15 min. The combined extract was purified by open column solid-liquid chromatography on 100–200 μm mesh size silica gel (Dickhut and Gustafson, 1995). Purified samples were quantified by injecting 2 μL of the extract into a Shimadzu QP5050A Gas Chromatograph/Mass Spectrometric Detector (GC/MS) in the selective ion monitoring mode. Column specifics as well as run conditions may be found in Hunsinger et al. (2008). Average recoveries for deuterated surrogate standards compared against deuterated internal standards for all samples were: $81.1 \pm 17.8\%$, $85.7 \pm 11.0\%$, and $93.0 \pm 11.6\%$; for d_{10} -anthracene, d_{12} -benzo(a)anthracene, and d_{12} -benzo(a)pyrene, respectively. The response of the GC/MS was verified by injecting a daily PAH relative response factor standard containing all PAHs analyzed; detected quantities of PAHs are only reported if the observed mass of PAH in a sample was greater than two times that observed in the laboratory sand blanks. The PAHs analyzed included phenanthrene (phen), anthracene (anth), 2-methylphenanthrene (2-MePhen), 2-methylanthracene (2-MeAnth), 1-methylanthracene (1-MeAnth), 1-methylphenanthrene (1-MePhen), fluoranthene (flu), pyrene (pyr), benzo[a]anthracene (b[a]a), chrysene (chry), benzo[b]fluoranthene (b[b]f), benzo[k]fluoranthene (b[k]f), benzo[e]pyrene (b[e]p), benzo[a]pyrene (b[a]p), perylene (peryl), and coronene (cor). All graphical and statistical analyses were conducted with either Microsoft Excel (2003 version) or Sigmaplot (v.10).

3. Results and discussion

3.1. Sedimentary and radiochemical character

X-radiographs and water content of sediment cores from the three study sites suggest that for Station 5-12A, a 12-cm-thick surficial layer of relatively transparent and high porosity silty clay rests above a normally graded basal sand layer (4–5 cm thick) (Fig. 2a). This layer rests on an irregular erosional surface incised into more highly consolidated strata (30% porosity). The upper

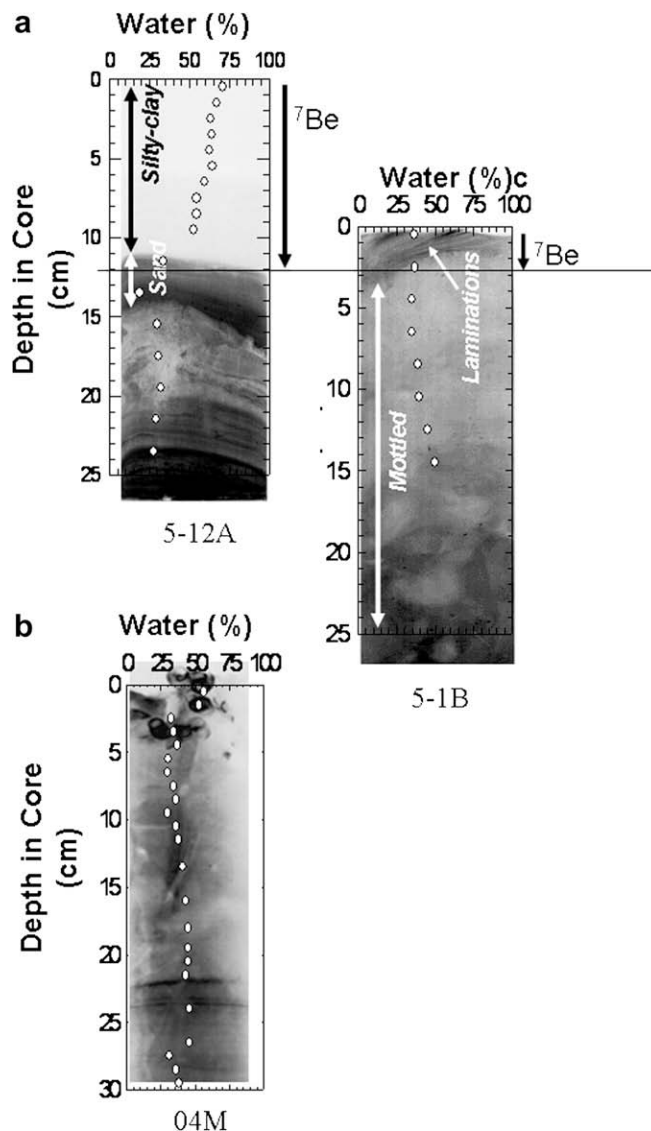


Fig. 2. X-radiograph images and water content for cores (a) 5-12A and 5-1B, and (b) core 04M. These X-radiographs are positives; lighter tones result from lower density such as mud and darker tones result from higher density such as sand and thicker shell. The erosional surface and visually observed mud layer goes down to ~12 cm in core 5-12A. Downcore water content (X-axis) is depicted by solid white circles. Solid line in Fig. 1a) demarcates depth of ^7Be penetration in core 12A and 1B, and by inference, the depth of hurricane-induced deposition.

layer in the X-radiograph original shows evidence of fine laminations (no bioturbation) that are not visible in Fig. 2a due to the large range in X-ray density reproduced in the figure. The presence of measurable ^7Be activity (53 d half-life) in the entire 12 cm surficial deposit (Fig. 2a) and preservation of the physical laminations suggests that the upper layer is post-storm (Sommerfield and Nittrouer, 1999). This pattern of upward event layer succession (incised surface – basal sand lag – laminated mud) is characteristic of hurricanes in Mississippi–Atchafalaya deltaic strata (Allison et al., 2007). The erosional surface is formed from wave-current erosion of the pre-storm seabed during storm maximum with the extent of the sand lag dependent on site-specific availability. The surficial mud layer, which often is subtly normally graded (Allison et al., 2007) – as is suggested by the rapid downcore decrease in porosity (Fig. 2a), is deposited during the waning phase with re-deposition of resuspended sediments. Station 5-12A also shows evidence of declining ^{210}Pb and ^{137}Cs activity in the surficial mud

layer toward the surface (Fig. 3) – the opposite of what would be expected from increasing clay content for radiotracer adsorption. Interestingly, the ^7Be inventories do decline with depth. This suggests that the source of the isotope results in its differences in inventory, since we interpret that layer deposition was rapid (\sim days). This upcore trend in the three isotopes at Station 5-12A is suggestive of initial shelf-derived sediment supply (relatively high Pb/Cs, low Be), followed by increasing supply of sediment runoff from near-shore areas in the post-storm draining away of floodwater with reduced Pb/Cs and increased Be activity. This should only be considered a general pattern as the waning phase event layer is likely a mixture of sediment from multiple source areas throughout the GOM and grain size also affects radioisotope activities.

Site 5-1B is a deeper (80 m water depth) site showing no obvious storm layer in the X-radiograph (Fig. 2a), albeit there is a minor laminated zone in the upper 3–5 cm. This is not surprising given that this is likely much deeper than the erosive storm wave-base. Sediments are generally mottled below this zone, indicative of extensive bioturbation. Beryllium-7 activity is confined to the upper 3 cm, and the ratio of Pb/Cs differs slightly in this laminated layer as well, relative to deeper sediment in this core (Fig. 3). Evidence of extensive bioturbation suggests that this core was collected in an area of low net sediment accumulation, which received \sim 3 cm of sediment in the waning-to-post-storm phase but no incision of pre-existing strata. Storm event layer thickness is reduced relative to Station 5-12A due to it being more distal from the incised inner shelf and terrestrial sediment sources. Influx of sediments and organic matter in these deep water areas of the GOM has been shown to be largely driven by stochastic events such as hurricanes and other wind and wave energy induced phenomenon (Corbett et al., 2007; Goni et al., 2007). For example, cores from sites surrounding Station 5-1B in similarly deeper re-

gions of the Gulf show rapid deposition of several cm-thick layers of sediment and associated materials in regions where long-term accumulation rates are typically low (\sim mm year $^{-1}$) (Corbett et al., 2007; Walsh et al., 2006). Thus, we cannot rule out the possibility that the upper 3 cm of this core is derived from the 2005 storms.

Core 04 M was collected in a freshwater *Panicum* marsh in the birdsfoot delta bordering the GOM (Fig. 1) that storm surge models (see <http://www.nd.edu/~adcirc/katrina.htm>) and site evidence (wrack lines) show was inundated by 3–4 m of water by the Katrina storm surge. The X-radiograph from Core 04 M contains physically laminated zones interspersed with massive intervals of bioturbation from macrofaunal burrows and root traces (Fig. 2b). A surficial gastropod layer is also present (Fig. 2b). While radioisotope activity was not quantified at this site, visual evidence of intact root mats and thin (<2 cm) and discontinuous sand deposits on the surface suggest limited erosional incision by the storm surge and limited deposition of waning phase mud. In summary, physical disturbance of the seabed from Hurricanes Katrina and Rita affected sediment deposition in the top \sim 10 cm of Core 5-12A, and possibly in the top \sim 2–3 cm of Core 5-1B, but did not contribute to sediment disturbances in Core 04 M.

3.2. Bulk organic matter

Organic matter in the Gulf of Mexico may be derived from *in situ* marine primary and secondary productivity, terrigenous and coastal plant-derived debris, or aged soil-derived organic matter from the watershed of the Atchafalaya and Mississippi Rivers (Goni et al., 1997). The downcore average OC abundance in cores 5-12A, 5-1B, and 04 M were $0.87 \pm 0.42\%$, $0.60 \pm 0.14\%$, and $1.03 \pm 0.18\%$, respectively (Fig. 4). Based on $\delta^{13}\text{C}_{\text{OC}}$, the composition of OC across all the sites appears to be a mixture of terrigenous and marine organic matter with $\delta^{13}\text{C}_{\text{OC}}$ being $-22.95 \pm 0.96\text{‰}$, $-23.12 \pm 0.14\text{‰}$, and $-24.66 \pm 0.81\text{‰}$ at Station 5-12A, 5-1B, and 04 M, respectively, and average downcore OC:N for each of these cores being 11.2 ± 1.3 , 10.89 ± 0.75 , and 12.7 ± 1.4 , respectively. Although the cores from all three sites display generally similar %OC, $\delta^{13}\text{C}$, and OC:N ratios, there is a marked contrast in sediment geochemistry above and below \sim 10 cm depth in the core from Station 5-12A; %OC, %N, $\delta^{13}\text{C}_{\text{OC}}$, and OC:N ratios all vary substantially in the top 10 cm of the core in contrast to the remainder of the core below this depth (Fig. 4, Supplementary Table S2). Organic matter in the top 10 cm of core 5-12A consists of relatively high levels of %OC that is enriched in ^{13}C and nitrogen. The bulk OM properties in the top 10 cm portion of core 5-12A are similar to pre-2005 hurricane OM found in surface sediments of the inner shelf of the GOM

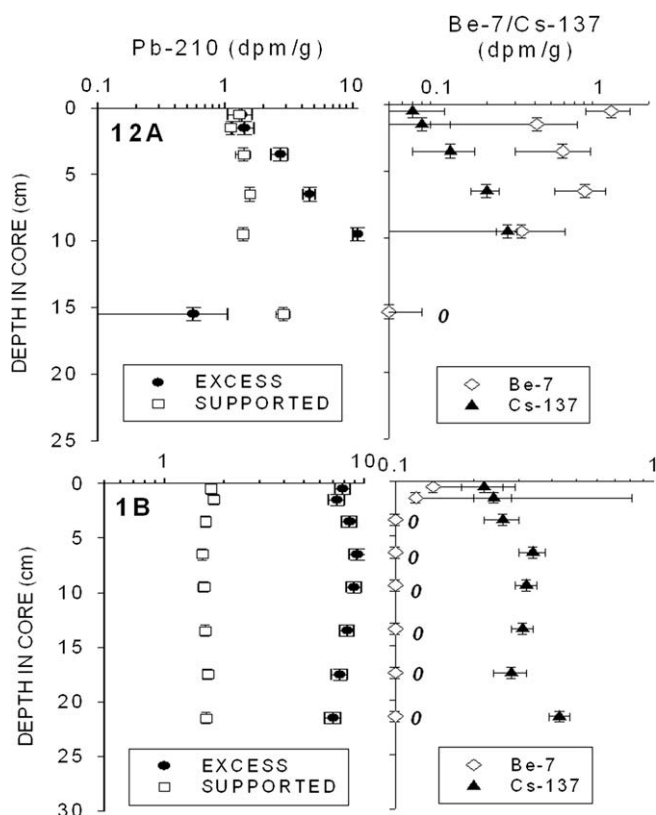


Fig. 3. Downcore radiochemistry data for cores 5-12A and 5-1B. Downcore depth for each graph in centimeters and activity of isotopes on the X-axis (dpm/g).

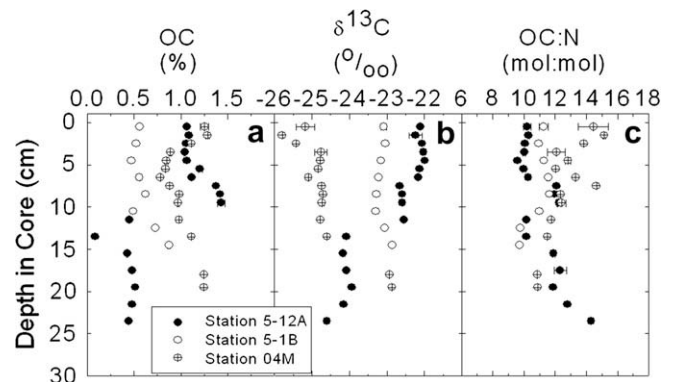


Fig. 4. Geochemical profiles of (a) percent organic carbon (%OC), (b) stable organic carbon isotopic signature, $\delta^{13}\text{C}_{\text{OC}}$ (‰) in relation to the PDB standard for each core, and (c) organic carbon to nitrogen ratio (OC:N). Note the deviation of values at beginning \sim 12 cm for core 5-12A.

from other stations (Gordon and Goni, 2003; Goni et al., 2007). A substantial reduction of $\delta^{13}\text{C}_{\text{OC}}$ by 2‰ is observed below 10 cm depth in the core, coincident with the depth at which major changes were noted visually in the X-radiograph and in sediment porosity (Fig. 2). The average $\delta^{13}\text{C}_{\text{OC}}$ of organic matter below 10 cm in core 5-12A ($-23.9 \pm 0.64\text{‰}$) is similar to values of $\delta^{13}\text{C}_{\text{OC}}$ in core 4 M from our study ($-24.7 \pm 0.81\text{‰}$) and in suspended sediments isolated from the lower Mississippi River as noted in another study ($-24.9 \pm 0.84\text{‰}$) (Bianchi et al., 2007). Elevated OC abundance along with enriched $\delta^{13}\text{C}_{\text{OC}}$, higher amounts of nitrogen enriched in ^{15}N , and lower OC:N ratios, are generally suggestive of inputs of marine organic matter (Hedges and Keil, 1995) to the top 10 cm of core 5-12A. With respect to bulk organic matter properties below 10 cm depth in core 5-12A, organic matter depleted in carbon and nitrogen and enriched in the heavier ^{13}C and ^{15}N isotopes, is indicative of vascular plants which use the C3 photosynthetic pathway (Cloern et al., 2002) that have been altered via weathering. We conclude that the sediments found below 10 cm in the core from Station 5-12A are comprised of such weathered material, introduced from aged C3 marsh material or aged soil material transported from the river's watershed to the shelf of the GOM.

Although ^7Be activity was detected in the top 3 cm of core 5-1B, bulk organic matter composition is fairly invariant throughout this core until about 10 cm depth (Fig. 4). Thus, bulk organic matter geochemical properties of sediments do not show a substantial difference above and below 3 cm, the perceived storm deposit per laminations in the X-radiograph image. Bulk organic matter properties change downcore in the core from Station 04 M, but as noted above, sediments at this site were not affected by mixing from the 2005 hurricanes. However, this is in contrast to marshes on the western side of the birdsfoot delta (<http://www.usgs.gov/newsroom/article.asp?ID=997>). Thus, the general trends in sediment geochemistry in the core from the marsh site are considered to be representative of local sources of organic matter (fluvial or marine) and *in situ* diagenesis, overlain with bioturbation and tidal mixing.

3.3. Polycyclic aromatic hydrocarbons

Downcore concentrations of individual PAHs are actually quite similar for all three cores, with a near surface peak in low to mid-molecular weight PAHs (MWt < 202) analyzed in all three cores (Fig. S1). Particulate phase concentrations of PAHs generally increase with the fraction of organic carbon associated with the particles (Schwarzenbach et al., 2003). In the case of our data, comparing concentrations of b[a]p, a high molecular weight PAH, with particulate OC content yielded a significant positive relationship ($r^2 = 0.47$; $p = 0.006$) for sediments in the core, but only for sediments in core 5-12A (see Fig. S2). Similar significant relationships were obtained between OC abundance and other high molecular weight PAHs in this core, suggesting that high molecular weight PAHs are associated closely with bulk OC in the core from Station 5-12A. In contrast, the overall lack of correlation between PAHs and OC abundance in the cores from Stations 5-1B and 04 M suggests that PAHs at these two sites may be associated with compositionally-specific portions of the overall particulate organic matter pool.

The significant correlation between bulk OC and high molecular weight PAHs in the core from Station 5-12A is important in the context of storm driven resuspension. Organic matter content of particles is likely to vary with grain size distribution, a function of sediment mixing. Specifically, we can “normalize” to particulate OC abundance to account for grain size effects due to sediment mixing from the 2005 storms and evaluate if the storm events are responsible for observed elevated PAH distributions in the

top portion of this core. In Table 1, we quantify the extent to which the 2005 storms affect PAH abundances in the core from 5-12A by comparing OC-normalized PAHs above 10 cm to those below 10 cm. For some of the PAHs quantified, normalization to sedimentary OC accounts for differences in that PAHs abundance above and below the storm layer (Table S3). For b[a]p, peryl, and cor, OC normalization results in a post-storm to pre-storm ratio of less than 1. In contrast, for other PAHs, sediments deposited in the storm layer were enriched 2 to 10 times, compared to pre-storm deposits of those same PAHs, respectively.

Isomer ratios of PAHs have been used to discriminate PAH sources ranging from urban to estuarine environments (Dickhut et al., 2000; Yunker et al., 2002). Comparing trends in isomer ratios over time, within a specific geographical setting, can be a powerful tool for diagnosing changes in historical influx of PAHs. Fig. 5 displays downcore ratios of (a) flu/flu+pyr, (b) b[a]a/b[a]a+chry, and (c) phenanthrene plus anthracene relative to their alkylated homologs (phen+anth/alkyl phen+alkyl anth) and shaded areas representing flu/flu+pyr and b[a]a/b[a]a+chry isomer ratios for lower Mississippi River surface water and bottom water suspended sediments. The variable pattern of isomer ratios in the top 10 cm of the core from 5-12A suggests that sources of PAHs throughout the hurricane deposit, while predominantly originating from petroleum and petroleum combustion (Fig. 5), are notably different from isomer ratios below the hurricane deposit. Below 10 cm depth, sedimentary PAHs seem to originate from a mixture of combustion sources. The average ratio of flu/flu+pyr and b[a]a/b[a]a+chry below 10 cm depth in core 5-12A is 0.49 ± 0.03 and 0.31 ± 0.05 , respectively. These ratios somewhat resemble isomer ratios from the top 14 cm of sediments from a pre-2005 study in which sediments were sampled for PAHs from stations in the inner shelf of the Gulf of Mexico (Turner et al., 2003). A station in that study (G50) located at ~ 90.10 longitude and ~ 28.70 latitude and in 50 water depth, is closest to station 5-12A. Ratios of flu/flu+pyr and b[a]a/b[a]a+chry at Station G50 were 0.44 ± 0.00 and 0.42 ± 0.02 , respectively (Turner et al., 2003). Although flu/flu+pyr in that study is somewhat similar to what we observe, the ratio of b[a]a/b[a]a+chry differs substantially from what we observe below 10 cm depth in core 5-12A. Comparing ratios of flu/flu+pyr and b[a]a/b[a]a+chry from other stations in the gulf close to our Station 5-12A (i.e. from 40 and 80 m water depth) (Turner et al., 2003) also yielded similar ratios of flu/flu+pyr (0.46 ± 0.03 and 0.51 ± 0.02 , respectively) but dissimilar ratios of b[a]a/b[a]a+chry suggesting that absolute comparisons of sedimentary b[a]a/b[a]a+chry to discriminate PAH sources may be imprudent in the GOM.

Although the data are scant for the core from Station 5-1B, PAH isomer ratios, specifically flu/(flu+pyr) vary widely in the top 5 cm of this core, indicating a range of PAH sources possibly stemming from a heterogeneous sediment deposition/mixing pattern. Below 5 cm, isomer ratios are more representative of a uniform source

Table 1
Ratios of organic carbon normalized PAHs in core 5-12A above 10 cm to those below 10 cm as an indicator of change in abundance due to the 2005 storms.

PAH	Ratio above 10 cm to below 10 cm
Anthracene	4.7
Fluoranthene	2.4
Pyrene	10.8
Benzo[a]anthracene	1.1
Chrysene	1.2
Benzo[b]fluoranthene	1.0
Benzo[k]fluoranthene	1.4
Benzo[a]pyrene	1.2
Benzo[a]pyrene	0.9
Perylene	0.5
Coronene	0.7

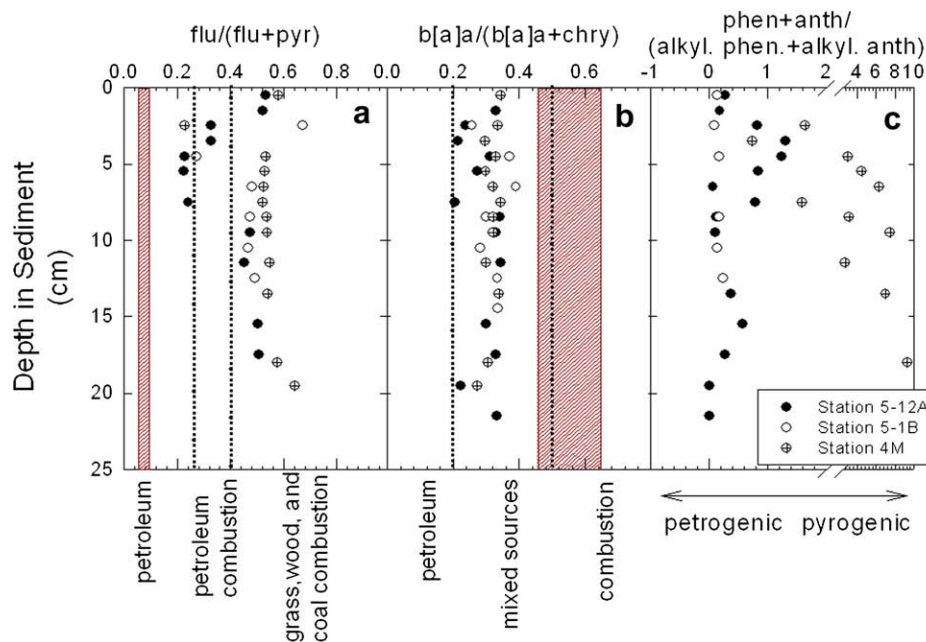


Fig. 5. Selected PAH isomer ratios in sediments indicative of PAH sources. PAH isomer ratio plots shown are (a) flu/(flu+pyr), (b) b[a]a/b[a]a+chry, and (c) sum of phenanthrene plus anthracene divided by the sum of their alkylated homologs. Symbols represent data from this work and shaded areas represent PAHs in lower Mississippi River suspended sediments from another study (Mitra and Bianchi, 2003). Phenanthrene was not detectable in lower Mississippi River particulates (Mitra and Bianchi, 2003); for this reason, there is no reference made to phenanthrene in the river in c.

of PAHs from a mixture of combustion processes. Downcore profiles flu/(flu+pyr) and b[a]a/b[a]a+chry in core 04 M are relatively invariant suggesting that isomer ratios at this marsh station have historically had a fairly consistent source of particulate phase PAHs deposited here. Also, ratios of phen+anth/alkyl phen+anth through the core from Station 04 M are much higher than at 5-12A and 5-1B (Fig. 5c), suggesting that PAHs at this station may have originated largely from combustion. This is in agreement with Iqbal et al. (2007), who show that pyrogenic PAHs influenced the PAH distributions in marsh areas around the delta prior to the 2005 hurricanes. The exception to this is a few discrete intervals in the top portion of this core, which are indicative of petroleum-derived PAH sources. Satellite imagery maps taken immediately after Hurricane Katrina have shown the presence of oil slicks proximal to the marsh area from which we obtained core 04 M (Rykhus, 2005).

In general, hurricanes in the GOM have been shown to resuspend and deposit large volumes of sediment into the seabed (Allison et al., 2005; Dail et al., 2007). Because we base our observations on three cores, we caution against extrapolating our data too far. But, our data from within these cores suggest that the 2005 hurricanes in the GOM may have remobilized pre-hurricane PAH-enriched sediment from the seabed in areas of relatively shallow water. In contrast, the core from the deeper offshore site and marsh site were seemingly protected from the storms. These observations are congruent with modeling of large storm activity on resuspension and re-emergence of buried sedimentary contaminants, which suggest that net resuspension of particulate phase contaminants from below the sediment water interface is a function of the balance between storm energy and net sediment accumulation at a site, the latter of which is related to the site's position on a continental margin (Niedoroda et al., 1996).

Acknowledgements

The authors acknowledge the assistance of Jeff Nittrouer and Carol Wilson from Tulane University and Bryan Fielder, Scott Hiller, Julie Manuel, Christian Noll, Jennifer Pitkewicz, and Marc Torres,

from TAMUG, for their assistance both in the field and lab. The captain and crew of R/V *Longhorn* are also acknowledged for their efforts in the field. The National Science Foundation – BES is acknowledged for providing a Small Grant for Exploratory Research to SM to conduct laboratory analyses. Funding for the rapid response study on the R/V *Longhorn* was from a supplementary grant through the Coastal Geosciences Program of the Office of Naval Research (ONR). We appreciate the efforts of Dr. Chuck Nittrouer at the University of Washington for serving as the ONR grant pass-through during a period when Tulane University was closed due to the storm.

Appendix A. Supplementary material

Supplementary data associated with this article can be found, in the online version, at doi:10.1016/j.marpolbul.2009.01.016.

References

- Achman, D.R., Brownawell, B.J., Zhang, L., 1996. Exchange of polychlorinated biphenyls between sediment and water in the Hudson River estuary. *Estuaries* 19 (4), 950–965.
- Allison, M.A., Sheremet, A., Goni, M.A., Stone, G.W., 2005. Storm layer deposition on the Mississippi–Atchafalaya subaqueous delta generated by Hurricane Lili in 2002. *Continental Shelf Research* 25 (18), 2213–2232.
- Allison, M.A., Dellapenna, T.M., Goni, M.A., Sheremet, A., 2007. Impact of Hurricanes Katrina and Lili on the inner shelf of the Mississippi–Atchafalaya delta. In: *Proceedings of the International Conference on Coastal Sediments 07*.
- Arzayus, K.M., Dickhut, R.M., Canuel, E.A., 2001. Fate of atmospherically deposited polycyclic aromatic hydrocarbons (PAHs) in Chesapeake Bay. *Environmental Science and Technology* 35 (11), 2178–2183.
- Bianchi, T.S., Pennock, J.R., Twilley, R.R., 1999. Biogeochemistry of Gulf of Mexico Estuaries: implications for management. In: Bianchi, T.S. (Ed.), *Biogeochemistry of Gulf of Mexico Estuaries*. John Wiley and Sons, New York.
- Bianchi, T.S., Wysocki, L.A., Stewart, M., Filley, T.R., McKee, B.A., 2007. Temporal variability in terrestrially-derived sources of particulate organic carbon in the lower Mississippi River and its upper tributaries. *Geochimica et Cosmochimica Acta* 71 (18), 4425–4437.
- Cloern, J.E., Canuel, E.A., Harris, D., 2002. Stable carbon and nitrogen isotope composition of aquatic and terrestrial plants of the San Francisco Bay estuarine system. *Limnology and Oceanography* 47, 713–729.

- Corbett, D.R., Dail, M.B., McKee, B.A., 2007. High frequency time-series of the dynamic sedimentation processes on the western shelf of the Mississippi River Delta. *Continental Shelf Research* 27, 1600–1615.
- Cutshall, N.H., Larsen, I.L., Olsen, C.R., 1983. Direct analysis of Pb-210 in sediment samples: self absorption corrections. *Nuclear Instruments and Methods* 206, 309–312.
- Dail, M.B., Corbett, D.R., Walsh, J.P., 2007. Assessing the importance of tropical cyclones on continental margin sedimentation in the Mississippi Delta region. *Continental Shelf Research* 27 (14), 1857–1874.
- Dickhut, R.M., Gustafson, K., 1995. Atmospheric inputs of selected polycyclic aromatic hydrocarbons and polychlorinated biphenyls to southern Chesapeake Bay. *Marine Pollution Bulletin* 30, 385–396.
- Dickhut, R.M. et al., 2000. Automotive sources of carcinogenic polycyclic aromatic hydrocarbons associated with particulate matter in the Chesapeake Bay region. *Environmental Science and Technology* 34, 4635–4640.
- Goni, M.A., Ruttenger, K.C., Eglinton, T.L., 1997. Sources and contribution of terrigenous organic carbon to surface sediments in the Gulf of Mexico. *Nature* 389, 275–278.
- Goni, M. et al., 2007. The effects of Hurricanes Katrina and Rita on the seabed of the Louisiana Shelf. *Sedimentary Record* 5, 1.
- Gordon, E.S., Goni, M.A., 2003. Sources and distribution of terrigenous organic matter delivered by the Atchafalaya River to sediments in the northern Gulf of Mexico. *Geochimica et Cosmochimica Acta* 67, 2359–2375.
- Harris, D., Horwath, W.R., van Kessel, C., 2001. Acid fumigation of soils to remove carbonates prior to total organic carbon or carbon-13 isotopic analysis. *Soil Science Society of America Journal* 65 (6), 1853–1856.
- Hedges, J.L., Keil, R.G., 1995. Sedimentary organic matter preservation: an assessment and speculative synthesis. *Marine Chemistry* 49 (2–3), 81–115.
- Hunsinger, G.B., Mitra, S., Warrick, J., Alexander, C.R., 2008. Oceanic loading of wildfire-derived organic compounds from a small mountainous river. *Journal of Geophysical Research – Biogeosciences* 113. doi:10.1029/2007JG000476.
- Iqbal, J., Gisclair, D., McMillin, D.J., Portier, R.J., 2007. Aspects of petrochemical pollution in southeastern Louisiana, USA: pre-Katrina background and source characterization. *Environmental Toxicology and Chemistry* 26, 2001–2009.
- Kennicutt II, M.C., Brooks, J.M., Atlas, E.L., Giam, C.S., 1988. Organic compounds of environmental concern in the Gulf of Mexico: a review. *Aquatic Toxicology* 11, 191–212.
- Macdonald, D.D., Carr, R.S., Calder, F.D., Long, E.R., Ingersoll, C.G., 1996. Development and evaluation of sediment quality guidelines for Florida coastal waters. *Ecotoxicology* 5, 253–278.
- Maruya, K.A., Loganathan, B.G., Kannan, K., McCumber-Kahn, S., Lee, R.F., 1997. Organic and organometallic compounds in estuarine sediments from the Gulf of Mexico. *Estuaries* 20, 700–709.
- Mitra, S., Bianchi, T.S., 2003. A preliminary assessment of polycyclic aromatic hydrocarbon distribution in the lower Mississippi River and Gulf of Mexico. *Marine Chemistry* 82, 273–288.
- Mitra, S., Dellapenna, T.S., Dickhut, R.M., 1999. Polycyclic aromatic hydrocarbon distribution within lower Hudson River estuarine sediments: physical mixing vs. sediment geochemistry. *Estuarine, Coastal, and Shelf Science* 49, 311–326.
- Niedoroda, A.W., Swift, D.J.P., Reed, C.W., Stull, J.K., 1996. Contaminant dispersal on the Palos Verdes continental margin: III. Processes controlling transport, accumulation, and re-emergence of DDT-contaminated sediment particles. *The Science of the Total Environment* 179, 109–133.
- Ogston, A.S., Cacchione, D.A., Sternberg, R.W., Kineke, G.C., 2000. Observations of storm and river flood-driven sediment transport on the northern California continental shelf. *Continental Shelf Research* 20 (16), 2141–2162.
- Overton, E.B., Ashton, B.M., Miles, M.S., 2004. Historical polycyclic aromatic and petrogenic hydrocarbon loading in Northern Central Gulf of Mexico shelf sediments. *Marine Pollution Bulletin* 49, 557–563.
- Parsons, M.L., 1998. Salt marsh sedimentary record of the landfall of Hurricane Andrew on the Louisiana coast: diatoms and other paleoindicators. *Journal of Coastal Research* 14 (3), 939–950.
- Rykhus, R.P., 2005. Satellite imagery maps Hurricane Katrina induced flooding and oil slicks. *Eos Transactions of the American Geophysical Union* 86, 381–382.
- Schwarzenbach, R.P., Gschwend, P.M., Imboden, D.M., 2003. *Environmental Organic Chemistry*. Wiley, Hoboken.
- Sommerfield, C.K., Nittrouer, C.A., 1999. Modern accumulation rates and a sediment budget for the Eel shelf: a flood-dominated depositional environment. *Marine Geology* 154, 227–241.
- Turner, R.E., Overton, E.B., Rabalais, N.N., Sen Gupta, B.K., 2003. Historical reconstruction of the contaminant loading and biological responses in the Central Gulf of Mexico shelf sediments. In: Service, U.-M.M. (Ed.), p. 140.
- Van Biersel, T.P., Carlson, D.A., Milner, L.R., 2007. Impact of hurricanes storm surges on the groundwater resources. *Environmental Geology* 53, 813–826.
- Walsh, J., Corbett, D.R., Mallinson, D., Goni, M., Dail, M.B., 2006. Mississippi Delta mudflow activity and 2005 Gulf Hurricanes. *Eos Transactions* 87 (44), 477.
- Yunker, M.B. et al., 2002. PAHs in the Fraser River basin: a critical appraisal of PAH ratios as indicators of PAH source and composition. *Organic Geochemistry* 33 (4), 489–515.